Supplementary Information

Exploring the role of chemical reactions in the selectivity of tyrosine kinase inhibitors

Mojgan Asadi, Wen Jun Xie, Arieh Warshel

Department of Chemistry, University of Southern California, Los Angeles, California 90089-1062, United States

1. Computational Methods

1.1 The Empirical Valence Bond (EVB) Method

We used the empirical valence bond (EVB) method to evaluate the proposed chemical steps of the catalytic activity in enzymes. The EVB is a QM/MM method where the chemical reactions are described by mixing the relevant diabatic states. The ith diabatic state constituting the EVB Hamiltonian has an energy

$$H_{ii} \equiv \epsilon_i = \alpha^i_{gas} + U^i_{intra}(r,q) + U^i_{Ss}(r, q, r', s) + U_{ss}(r',q'), \#(S1)$$

where r and q are, respectively, the atomic coordinates and partial charges of a region of the reacting fragments (solute/region 1) in the ith diabatic basis, and r' and q' are the positions and charges of the rest of the system (solvent/region 2). The various energy contributions are as follows: α^i_{gas} is the gas-phase energy, $U^i_{intra}(r,q)$ is the region 1 intramolecular potential, $U_{ss}(r',q')$ is the region 2 potential, and $U^i_{Ss}(r, q, r', s)$ is the interaction between the two regions.

We performed our EVB calculations using the Q6 software package[1] and the AMBER force field[2] for region 2 atoms. The standard ff14sb force field was used for protein atoms[3]. The force field parameters for atoms in the non-covalent and covalent ligands were determined from the GAFF force field using Ambertools[4]. Bond breaking and forming within region 1 is modeled using a Morse potential

$$V_b = D_M \left[1 - e^{a(b - b_0)}\right]^2, \#(S2)\#$$

where b is the bond length between the atoms, b_0 is the equilibrium bond length, a controls the effective equilibrium force constant, and D_M is the bond dissociation energy.

The EVB free energy surfaces are calculated with FEP/umbrella sampling using linear combinations of the diagonal Hamiltonian energies as mapping potentials. For a reaction going from an initial state 1 to a final state 2, this potential has the form

$$\epsilon_m = \lambda_m \epsilon_1 + (1 - \lambda_m)\epsilon_2, \#(S3)$$

where $0 \leq \lambda_m \leq 1$ guides the potential from state 1 to state 2. The differential free energy in a single sampling window of the guiding potential is

$$\delta G(\lambda_m \rightarrow \lambda_{m+1}) = -kT \ln \left[\left\langle e^{-\frac{\epsilon_{m+1} - \epsilon_m}{kT}} \right\rangle_m\right] \#(S4)$$

which is integrated to the free energy surface of the guiding potential

$$\Delta G(\lambda_n) = \Delta G(\lambda_0 \rightarrow \lambda_n) = \sum_{i=0}^{n-1} \delta G(\lambda_i \rightarrow \lambda_{i+1}). \#(S5)$$

We use umbrella sampling to obtain the free energy surface $\Delta G(X_n)$ of the reaction coordinate, which we take to be the energy gap $\Delta\epsilon = \epsilon_1 - \epsilon_2$.

$$\exp\left[-\Delta G(X^n)/kT\right] = \exp\left[-\Delta G(\lambda_m)/kT\right]\left\langle \exp\left[-(\epsilon_m(X^n) - E_g(X^n))/kT\right]\right\rangle_m \ \#(S6)$$

where $E_g(X_n)$ is the ground state energy of the EVB Hamiltonian matrix. Here ϵ_m is the mapping potential that keeps X near X^n.

The EVB parameters used in our simulations are tabulated in Schemes S3-S14.

1.2 Protein Dipole Langevin Dipole (PDLD)

The evaluation of the protein-ligand binding free energies in this study done using the semi-macroscopic protein dipole Langevin dipole (PDLD-S) method, using the linear response approximation (PDLD/S-LRA/β)[5]. The electrostatic contribution is evaluated within the LRA formulation by averaging the protein-ligand electrostatic energy over trajectories that are propagated on the potentials of both the polar and non-polar states of the ligand[6]. The PDLD calculation was done using the Polaris module of MOLARIS-XG[7]. The scaling of the non-electrostatic term was increased by 0.5. The system is embedded in a 16 Å simulation sphere centered around the acalabrutinib inhibitor and surrounded by a bulk continuum. The electrostatic interactions were treated by the Local Reaction Field (LRF) method[8]. The electrostatic binding PDLD energies was averaged over 21 different configurations equilibrated for 20ps.

1.3 Time-dependent kinetic simulations

The kinetic simulations of the BTK and ITK with the acalabrutinib inhibitor was done using Mathematica[9]. The reaction schemes of Eqs. 1 and 2 in the main text were implemented as systems of ordinary differential equations and numerically solved for the given initial conditions at varying initial concentrations of inhibitor. Integration of the ODEs yields an observable product concentration $[\mathrm{P}](t)$ as well as the product formation velocity $v(t) = \frac{d[\mathrm{P}]}{dt}$. After a long time, the product formation velocity follows an effective exponential decay $v(t) \approx v_i e^{-k_{obs}t}$, where v_i is the initial velocity of product formation and k_{obs} is the observed effective (pseudo-first order) rate constant of product formation. This rate is calculated from our kinetic simulations using

$$k_{calc} = -(\ln v(T + \Delta t) - \ln v(T))/\Delta t \ \#(S7)$$

where T is a sufficiently large amount of time to allow $v(t)$ to exhibit linear behavior on a semi-log scale, and Δt is small compared to T. We then obtain k_{calc} for different initial concentrations $[\mathrm{I}]_0$. In the limit of small inhibitor concentrations, we expect k_{calc} to follow the linear behavior

$$k_{calc} = \frac{\frac{k_{inac}}{K_i}}{1 + \frac{K_m}{[S]_0}} [I]_0, \#(S8)$$

which we use to extract the calculated $k_{eff} = k_{inact}/K_i$ of the simulated assay.

The inhibition fraction $[EI]/[E]_0$ is also plotted at different times as a function of log initial concentration of the inhibitor. The intersection of the inhibition curves with the half-fraction line allows us to infer the time-dependent $IC50(t)$. We are primarily interested in observing its long-time behavior at approximately sub μM concentrations.

2. EVB Parameters and alternative reaction mechanisms

The complete set of reaction pathways attempted for BTK and ITK are summarized in Schemes S1 and S2 and illustrated in Figures 1 and 2. We explored different pathways in ITK that include the possibility of a chemically involved aspartate residue. However, such pathways consistently result in a higher overall barrier in protein. Schemes S3-S10 illustrate all individual possible steps for the ITK schemes and tabulate their EVB parameters. Likewise, Figures S11-S14 illustrate the steps for the BTK schemes and tabulate their corresponding EVB parameters.

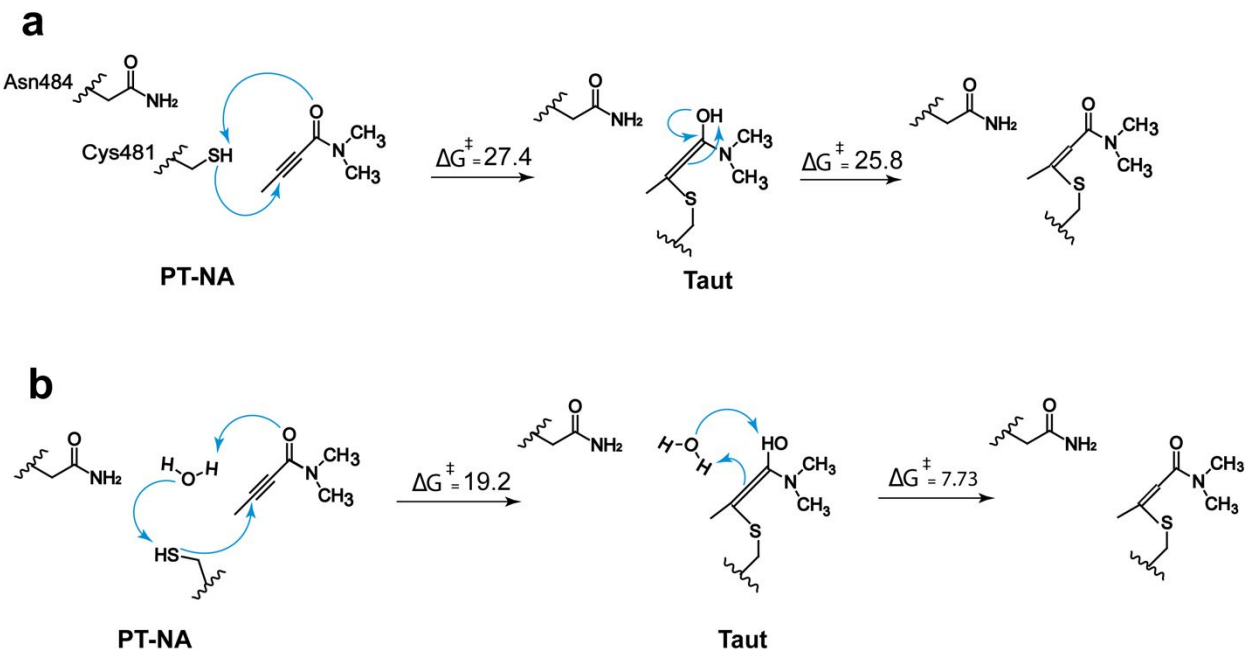

Scheme S1. Summary of all attempted catalytic reaction paths and their barriers in BTK enzyme, where the free energy measured in kcal/mol.

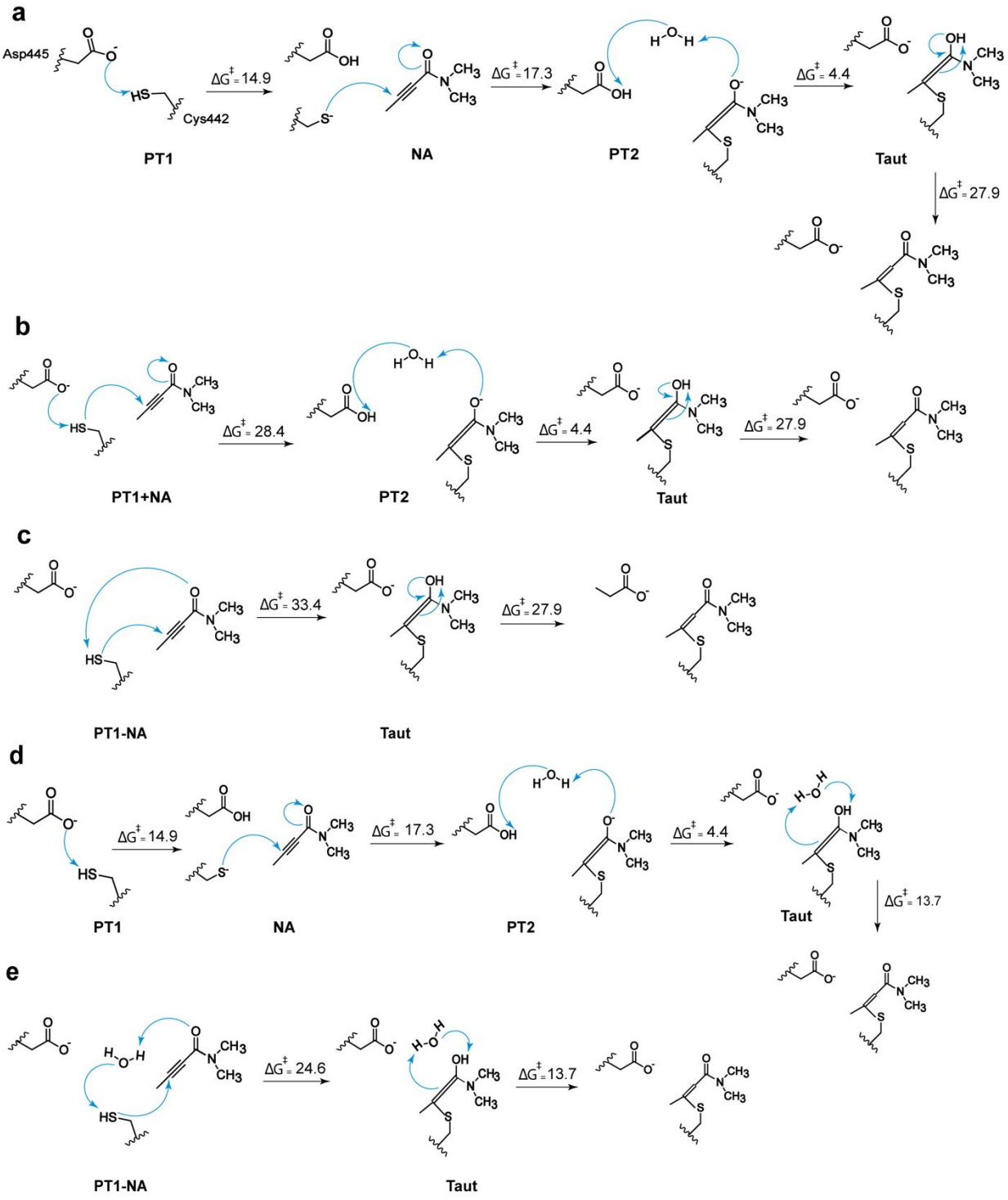

Scheme S2. Summary of all attempted catalytic reaction paths and their barriers in ITK enzyme, where the free energy measured in kcal/mol.

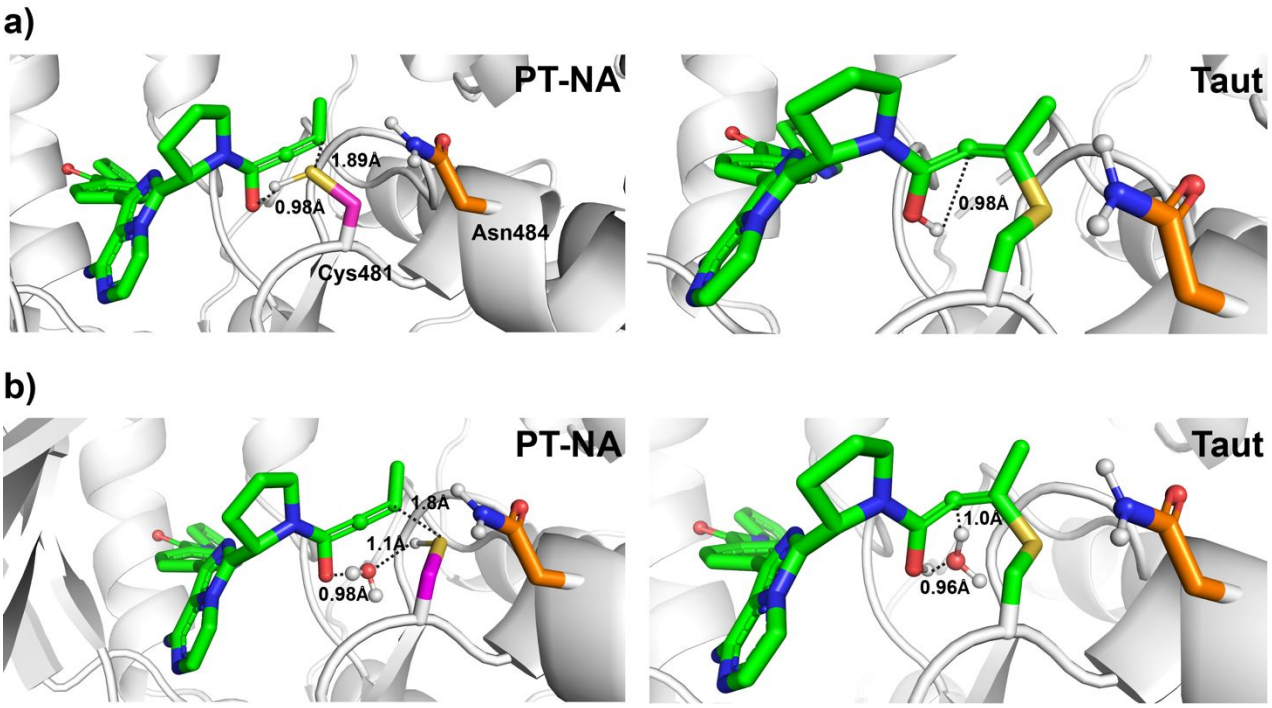

Figure S1. Illustration of reaction mechanism steps for BTK shown in scheme S1, which include proton transfer (PT), nucleophilic attack (NA), and tautomerization (Taut) steps.

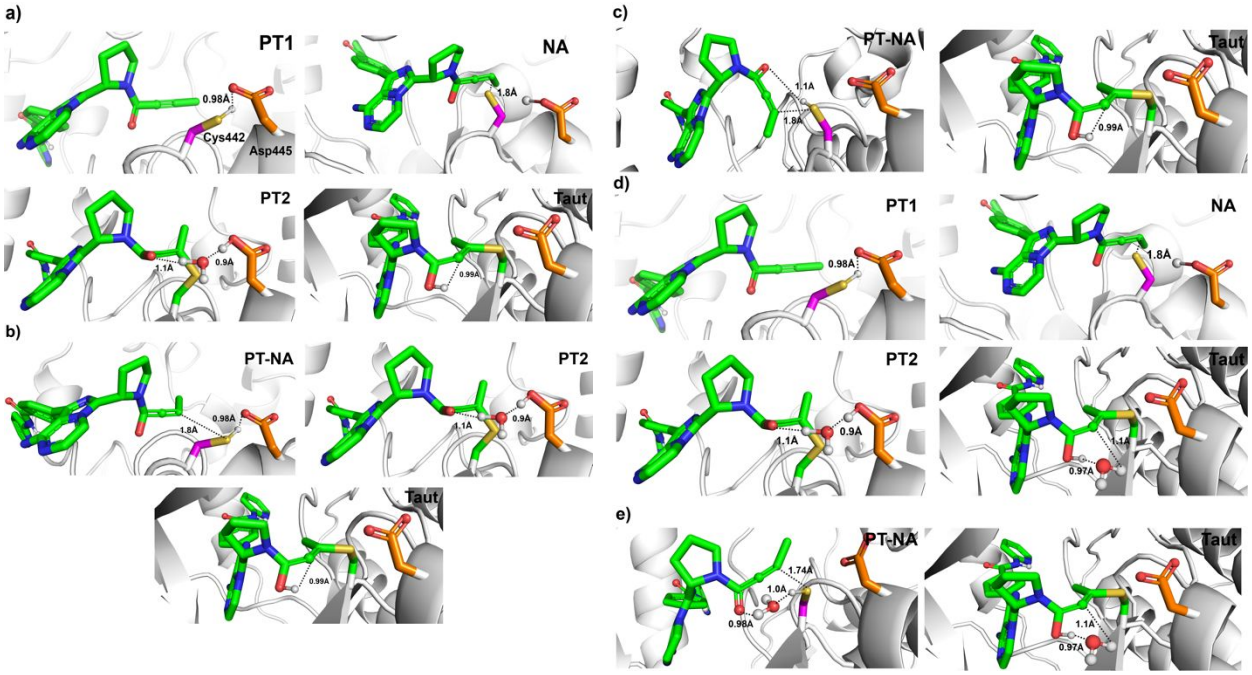

Figure S2. Illustration of reaction mechanism steps for ITK shown in scheme S2, which include proton transfer (PT), nucleophilic attack (NA), and tautomerization (Taut) steps.

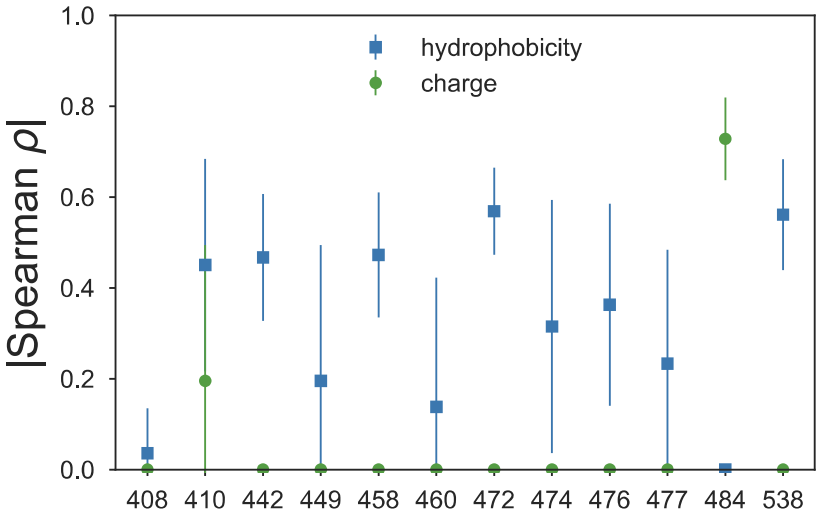

Figure S3. Spearman correlation between the IC50 and the characteristics of each non-conserved residue in the tyrosine kinases' active site. Considered are twelve residues. Each residue's formal charge and hydrophobicity are regarded as features. BTK is used for residue numbering. The hydrophobicity scale is obtained from ref [10].

Enzyme	Parameter	Value	Source
BTK	K_m	150 μM	Reference 13.
	$k_{\text{eff,cat}}$	$3.7 \times 10^{-3}\ \text{s}^{-1}\ \mu\text{M}^{-1}$	Reference 12.
	k_s	$0.05\ \text{s}^{-1}\ \text{nM}^{-1}$	Estimate
	$[\text{S}]_0$	300 μM	Reference 13.
ITK	K_m	36 μM	Reference 11.
	$k_{s,\text{cat}}$	0.0105 s^{-1}	Reference 11.
	k_s	$0.1\ \text{s}^{-1}\ \text{nM}^{-1}$	Estimate
	$[\text{S}]_0$	100 μM	Reference 13.

Table S1. Kinetic parameters for the catalytic process used in kinetic simulations, in which the process of ATP binding and phosphorylation is approximated by Michaelis-Menten kinetics[11–13]. The kinetic equation is completely determined using $k_{\text{inact}} = k_{\text{eff}} * K_i$ and $k_{-1,\text{cat}} = K_m k_1 - k_{s,\text{cat}}$.

Enzyme	Parameter	Value	Source
BTK	K_i	60 nM	Estimate
	k_{eff}	$3.0 \times 10^{-5}\ \text{s}^{-1}\ \text{nM}^{-1}$	Reference 13.
	k_1	$0.1\ \text{s}^{-1}\ \text{nM}^{-1}$	Estimate
	$[\text{E}]_0$	5 nM	Reference 13.
ITK	K_i	10,000 nM	Estimate
	k_{eff}	$7 \times 10^{-9}\ \text{s}^{-1}\ \text{nM}^{-1}$	Reference 13.
	k_1	$0.1\ \text{s}^{-1}\ \text{nM}^{-1}$	Estimate
	$[\text{E}]_0$	5 nM	Reference 13.

Table S2. Kinetic parameters for the inhibition process used in the kinetic simulations of experimental assays using Eq. (1) in the main text. We estimated K_i to obtain dynamics closely resembling Liclican (2020)[13]. We additionally estimated $k_1 = 0.1\ \text{s}^{-1}\ \text{nM}^{-1}$ for both enzymes, which has no bearing on long-time dynamics. The kinetic equation is completely determined using $k_{\text{inact}} = k_{\text{eff}} K_i$ and $k_{-1} = k_1 K_i$.

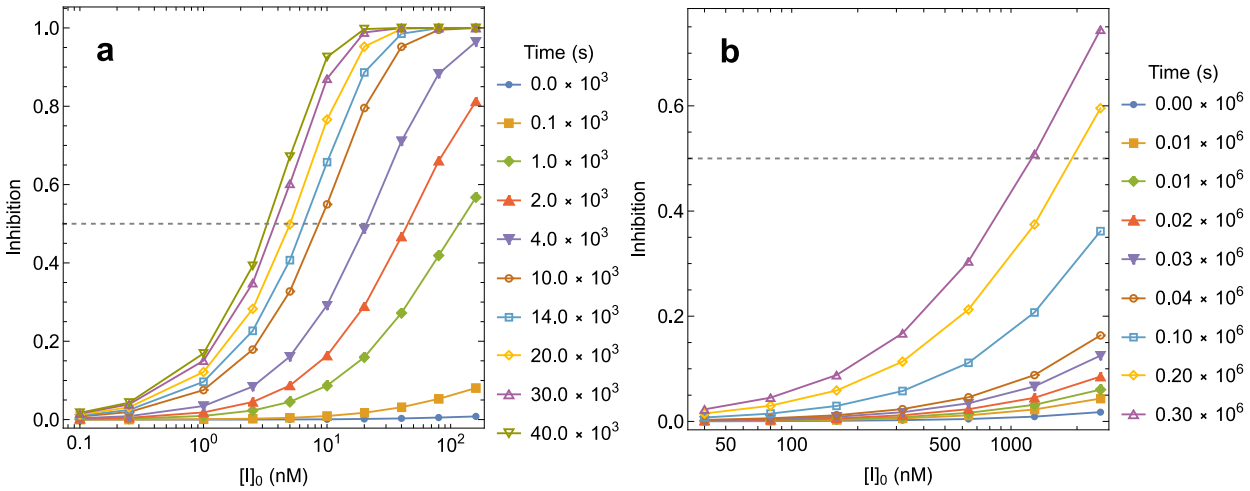

Figure S4. Simulation of experimental assay conditions using the parameters and initial conditions in Tables S1 and S2, simulating the experimental procedure in Liclican (2020)[13] for (a) BTK and (b) ITK enzyme assays.

Scheme S3

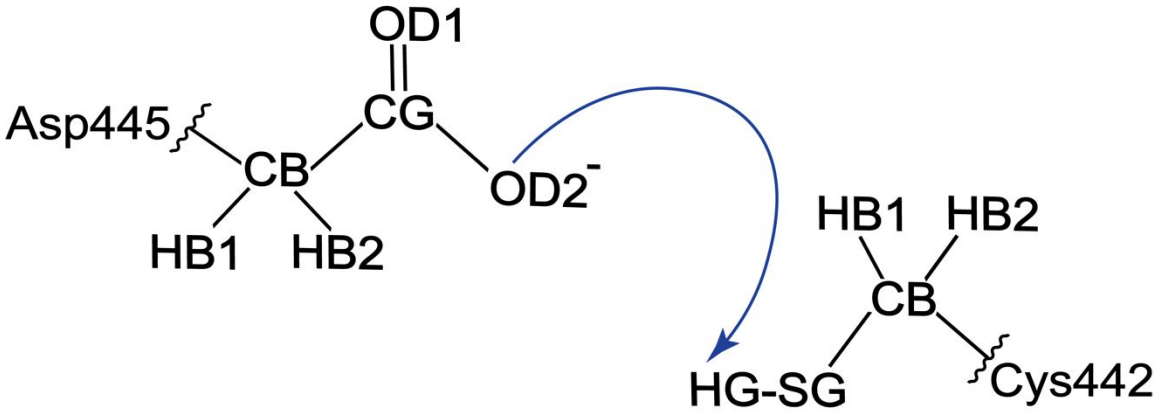

Scheme S3 Figure. The first proton transfer (PT1) from aspartic acid 445 to cysteine 442, appearing in scheme S2 (a) and (d)

Scheme S3 Table. Atomic charges used for the first proton transfer in ITK from cysteine 442 to aspartic acid 445.

Systems	Atom	RESP charges in RS state	Atom type (RS)	RESP charges in PS state	Atom type (PS)
Cysteine	CB	-0.109	2C	0.078	CT
	HB1	0.126	H1	0.039	H1
	HB2	0.126	H1	0.039	H1
	SG	-0.414	SH	-1.117	SH
	HG	0.263	HS	0.539	HO
Aspartic acid	CB	-0.457	2C	-0.544	2C
	CG	1.181	CO	1.073	C
	OD1	-1.021	O2	-0.745	O
	OD2	-1.021	O2	-0.729	OH
	HB1	0.140	HC	0.202	HC
	HB2	0.140	HC	0.202	HC

Calibration			
H_{12}		α	
4.78		80.44	
Atom Type			
Atom type	**LJ Rm**	**LJ_eps**	**SP_Ci**
SH	2.0	0.25	91
HS	0.6	0.0157	50
HO	0.0	0.0	50
O2	1.66	0.21	91
OH	1.72	0.21	50
Bond Type			
PRM_ID	**D(kcal/mol)**	**alpha**	**r0**
HS-SH	94.0	1.4	1.345
HO-OH	102.0	2.35	0.960

Scheme S4

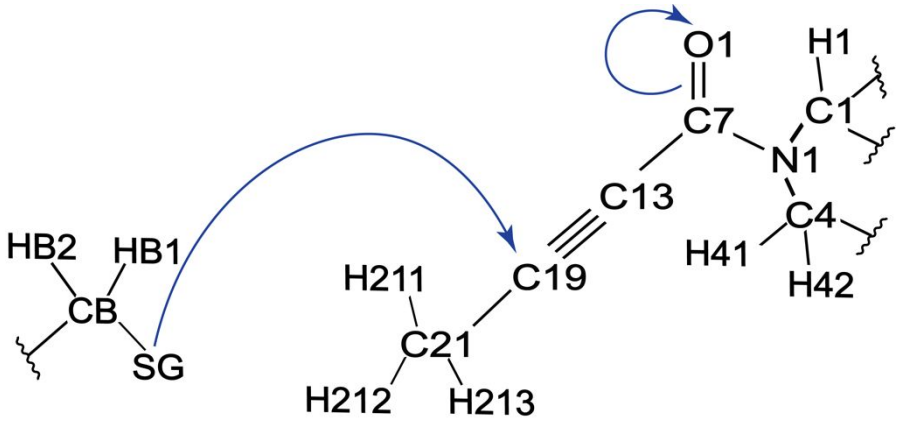

Scheme S4 Figure. The Nucleophilic acid (NA) step between cysteine 442 and C19 of inhibitor, in scheme S2 (a) and (d).

Scheme S4 Table. Atomic charges used in ITK for the nucleophilic attack between the sulfur of cysteine 442 and the carbon C19 carbon of the inhibitor.

Systems	Atom	RESP charges in RS state	Atom type (RS)	RESP charges in PS state	Atom type (PS)
Cysteine	CB	0.078	CT	0.0785	c3
	HB1	0.039	H1	0.179	h1
	HB2	0.039	H1	0.179	H1
	SG	-1.118	S	-0.448	ss
Inhibitor	C21	-0.335	c3	-0.206	c3
	H211	0.189	hc	0.074	hc
	H212	0.189	hc	0.074	hc
	H213	0.189	hc	0.074	hc
	C19	0.315	c1	0.815	c2
	C13	-0.599	cg	-1.495	c1
	C7	0.996	c	1.209	c2
	O1	-0.795	o	-0.858	o
	N1	-0.059	n	-0.253	n
	C4	-0.336	c3	-0.329	c3
	H41	0.193	h1	0.189	h1
	H42	0.193	h1	0.189	h1
	C1	-0.336	c3	0.329	c3
	H1	0.193	h1	0.189	h1

Calibration			
H_{12}		α	
61.77		130.51	
Atom Type			
Atom_type	**LJ_Rm**	**LJ_eps**	**SP_Ci**
S	2.0	0.25	30
ss	2.0	0.25	90
c1	1.9	0.0157	91
c2	1.9	0.21	91
Bond Type			
PRM_ID	**D(kcal/mol)**	**alpha**	**r0**
c2-ss	90.0	1.4	1.86

Scheme S5

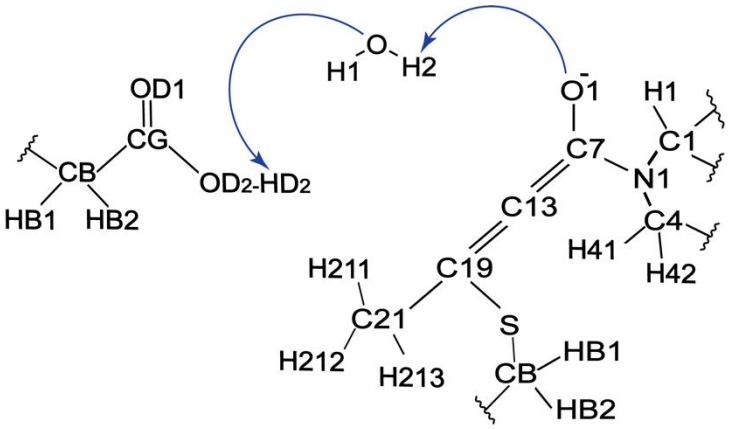

Scheme S5 Figure. The second proton transfer (PT2) from aspartic acid 445 to water and from water to inhibitor, corresponding to scheme S2 (a), (b), and (d).

Scheme S5 Table. Atomic charges used for the second proton transfer in ITK from water to inhibitor and from aspartic acid to water.

Systems	Atom	RESP charges in RS state	Atom type (RS)	RESP charges in PS state	Atom type (PS)
Cysteine	CB	-0.255	c3	-0.367	c3
	HB1	0.179	h1	0.201	h1
	HB2	0.179	h1	0.201	h1
	SG	-0.448	ss	-0.195	ss
Inhibitor	C21	-0.206	c3	-0.713	c3
	H211	0.075	hc	0.250	hc
	H212	0.075	hc	0.250	hc
	H213	0.075	hc	0.250	hc
	C19	0.816	c2	0.336	c2
	C13	-1.495	c1	-0.351	c1
	C7	1.208	c2	0.600	c2
	O1	-0.858	o	-0.717	oh
	N1	-0.253	n	-0.406	nh
	C4	-0.329	c3	-0.146	c3
	H42	0.189	h1	0.140	h1
	H43	0.189	h1	0.140	h1
	C1	-0.329	c3	-0.146	c3
	H1	0.189	h1	0.140	h1
Aspartic acid	CB	-0.544	2C	-0.457	2C
	CG	1.074	C	1.181	CO
	OD1	-0.745	O	-1.022	O2
	OD2	-0.729	OH	-1.022	O2
	HB1	0.202	HC	0.140	HC
	HB2	0.202	HC	0.140	HC
	HD2	0.538	HO	0.417	HW
Water	O	-0.834	OW	-0.834	OW
	H1	0.417	HW	0.417	HW
	H2	0.417	HW	0.531	ho

Calibration	
H_{12}	α
26.64	-21.07

Atom Type			
Atom_type	**LJ_Rm**	**LJ_eps**	**SP_Ci**
o	1.66	0.21	91
oh	1.72	0.21	50
O2	1.66	0.21	91
OH	1.72	0.21	50
HO	0.0	0.0	50
HW	0.0	0.0	50
OW	1.76	0.152	53
ho	0.0	0.0	50

Bond Type			
PRM_ID	**D(kcal/mol)**	**alpha**	**r0**
HW-OW	97.2	2.0	0.988
HO-OH	102.0	2.0	0.988
Ho-oh	102.0	2.0	0.988

Scheme S6

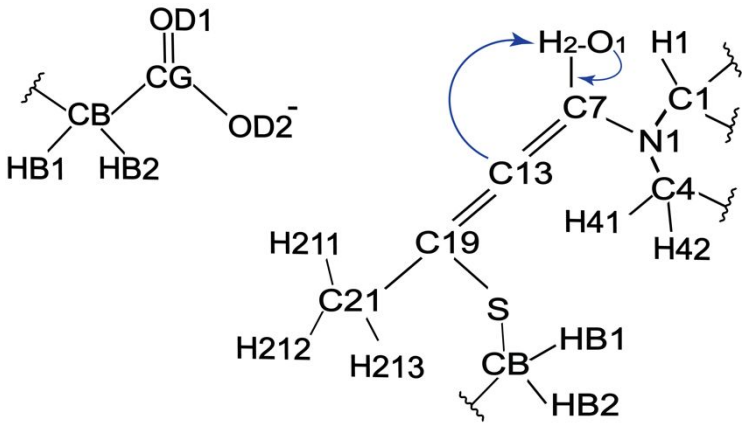

Scheme S6 Figure. The direct tautomerization step appearing in schemes S1 (a) and S2 (a)-(c).

Scheme S6 Table. Atomic charges used for the direct tautomerization reaction, the proton transfer through the inhibitor in ITK.

Systems	Atom	RESP charges in RS state	Atom type (RS)	RESP charges in PS state	Atom type (PS)
Inhibitor	CB	-0.367	c3	-0.278	c3
	HB1	0.201	h1	0.197	h1
	HB2	0.201	h1	0.197	h1
	SG	-0.195	ss	-0.225	ss
	C21	-0.713	c3	-0.339	c3
	H211	0.250	hc	0.161	hc
	H212	0.250	hc	0.161	hc
	H213	0.250	hc	0.161	hc
	C19	0.336	c2	0.368	c2
	C13	-0.351	c1	-0.579	ce
	C7	0.601	c2	0.904	c
	O1	-0.717	oh	-0.799	o
	N1	-0.406	nh	-0.051	n
	C4	-0.146	c3	-0.403	c3
	H42	0.140	h1	0.212	h1
	H43	0.140	h1	0.212	h1
	C1	-0.146	c3	-0.406	c3
	H1	0.140	h1	0.212	h1
	H2	0.531	ho	0.292	ha

Calibration			
H_{12}		α	
2.75		-89.38	
Atom Type			
Atom_type	**LJ_Rm**	**LJ_eps**	**SP_Ci**
c1	1.9	0.21	53
ce	1.9	0.089	53
oh	1.72	0.21	53
o	1.66	0.21	50
ho	0.0	0.0	50
Bond Type			
PRM_ID	**D(kcal/mol)**	**alpha**	**r0**

ho-oh	102.0	2.0	0.988
ce-ha	100.0	2.3	1.1

Scheme S7

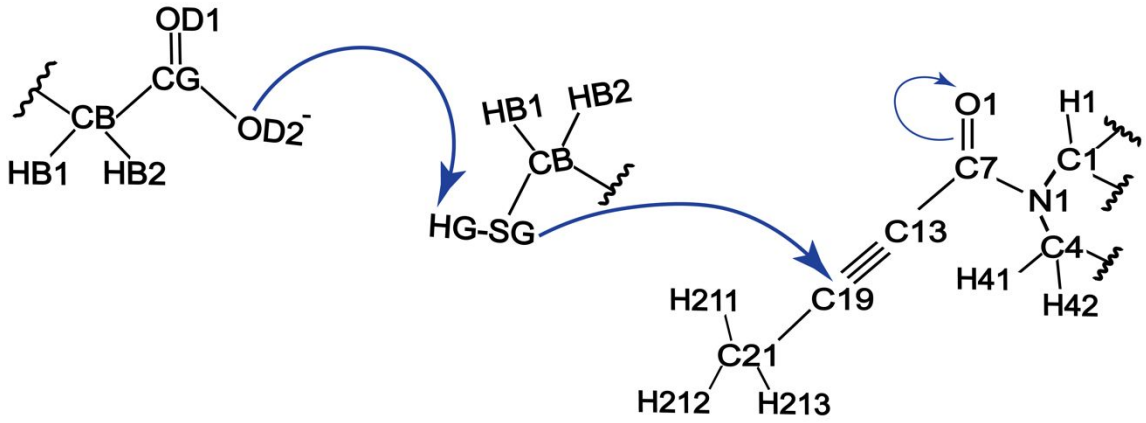

Scheme S7 Figure. The concerted proton transfer and nucleophilic attack step corresponding to scheme S2 (b).

Scheme S7 Table. Atomic charges used for the first proton transfer between cysteine 442 and aspartic acid 445 and the nucleophilic attack between sulfur of cysteine and C19 of inhibitor in ITK.

Systems	Atom	RESP charges in RS state	Atom type (RS)	RESP charges in PS state	Atom type (PS)
Cysteine	CB	-0.116	2C	-0.255	c3
	HB1	0.117	H1	0.179	h1
	HB2	0.117	H1	0.179	h1
	SG	-0.391	SH	-0.448	ss
	HG	0.267	HS	0.536	HO
Aspartic acid	CB	-0.463	2C	-0.545	2C
	CG	1.195	CO	1.093	C
	OD1	-0.992	O2	-0.737	O
	OD2	-0.992	O2	-0.722	OH
	HB2	0.124	HC	0.184	HC
	HB3	0.124	HC	0.184	HC
Inhibitor	C21	-0.336	c3	-0.205	c3
	H211	0.189	hc	0.075	hc
	H212	0.189	hc	0.075	hc
	H213	0.189	hc	0.075	hc
	C19	0.316	c1	0.816	c2
	C13	-0.599	cg	-1.494	c1
	C7	0.996	c	1.208	c2
	O1	-0.795	o	-0.858	o
	N1	-0.056	n	-0.253	n
	C4	-0.336	c3	-0.329	c3
	H42	0.193	h1	0.189	h1
	H43	0.193	h1	0.189	h1
	C1	-0.336	c3	-0.329	c3
	H1	0.193	h1	0.189	h1

Calibration			
H_{12}		α	
65.23		213.03	
Atom Type			
Atom_type	**LJ_Rm**	**LJ_eps**	**SP_Ci**
SH	2.0	0.25	53

ss	2.0	0.25	91
HS	0.6	0.015	53
HO	0.0	0.0	53
O2	1.66	0.21	90
OH	1.72	0.21	50
c1	1.9	0.21	91
c2	1.9	0.086	91
Bond Type			
PRM_ID	**D(kcal/mol)**	**alpha**	**r0**
HS-SH	94.0	1.4	1.345
HO-OH	102.0	2.0	0.988
c2-ss	90.0	1.2	1.86

Scheme S8

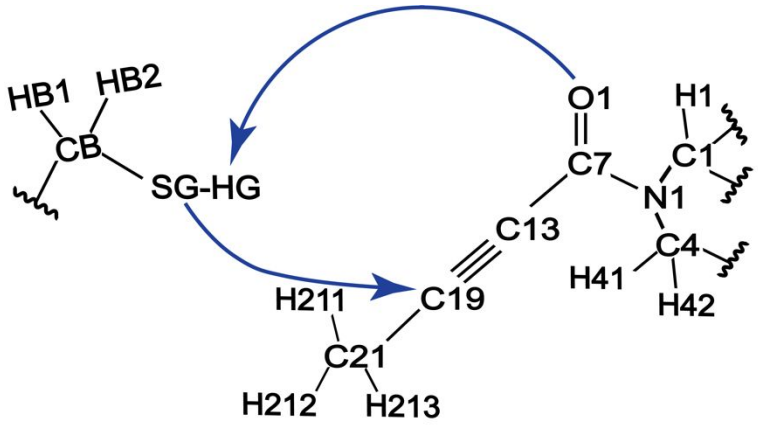

Scheme S8 Figure. The direct proton transfer and nucleophilic attack step corresponding to scheme S2 (c).

Scheme S8 Table. Atomic charges used for the first proton transfer between cysteine 442 and O1 atom of inhibitor and the nucleophilic attack between sulfur of cysteine and C19 of inhibitor in ITK.

Systems	Atom	RESP charges in RS state	Atom type (RS)	RESP charges in PS state	Atom type (PS)
Cysteine	CB	-0.109	2C	-0.367	c3
	HB1	0.126	H1	0.201	h1
	HB2	0.126	H1	0.201	h1
	SG	-0.414	SH	-0.195	ss
	HG	0.262	HS	0.531	HO
Inhibitor	C21	-0.336	c3	-0.713	c3
	H211	0.189	hc	0.251	hc
	H212	0.189	hc	0.251	hc
	H213	0.189	hc	0.251	hc
	C19	0.316	c1	0.336	c2
	C13	-0.599	cg	-0.351	c1
	C7	0.996	c	0.601	c2
	O1	-0.795	o	-0.717	o
	N1	-0.057	n	-0.406	n
	C4	-0.336	c3	-0.146	c3
	H42	0.193	h1	0.140	h1
	H43	0.193	h1	0.140	h1
	C1	-0.336	c3	-0.146	c3
	H1	0.193	h1	0.140	h1

Calibration			
H_{12}		α	
36.78		208.89	
Atom Type			
Atom_type	**LJ_Rm**	**LJ_eps**	**SP_Ci**
SH	2.0	0.25	30
ss	2.0	0.25	90
HS	0.6	0.0157	50
HO	0.0	0.0	50
O2	1.66	0.21	90
OH	1.7	0.21	50

c1	1.908	0.21	91
c2	1.908	0.089	91
Bond Type			
PRM_ID	**D(kcal/mol)**	**alpha**	**r0**
HS-SH	94.0	1.4	1.345
HO-OH	102.0	2.0	0.988
c2-ss	90.0	1.2	1.86
Improper_types			
Index	**Fc**	**phi0**	**PRM_ID**
3	10.5	180.0	Cg-c-n-0

Scheme S9

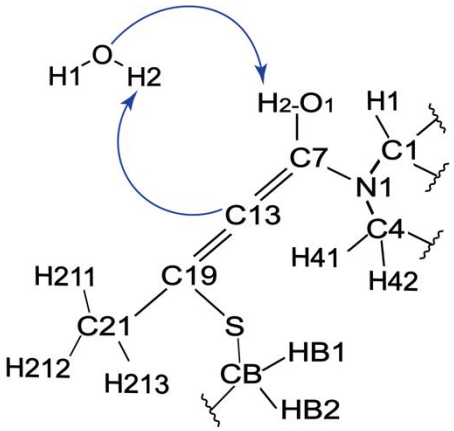

Scheme S9 Figure. The solvent assisted tautomerization step corresponding to scheme S2 (d).

Scheme S9 Table. Atomic charges used for solvent assisted tautomerization in ITK.

Systems	Atom	RESP charges in RS state	Atom type (RS)	RESP charges in PS state	Atom type (PS)
Inhibitor	CB	-0.367	c3	-0.278	c3
	HB1	0.201	h1	0.197	h1
	HB2	0.201	h1	0.197	h1
	SG	-0.195	ss	-0.225	ss
	C21	-0.713	c3	-0.339	c3
	H211	0.251	hc	0.162	hc
	H212	0.251	hc	0.162	hc
	H213	0.251	hc	0.162	hc
	C19	0.335	c2	0.368	c2
	C13	-0.351	c1	-0.579	ce
	C7	0.601	c2	0.904	c
	O1	-0.717	oh	-0.798	o
	N1	-0.406	nh	-0.051	n
	C4	-0.146	c3	-0.403	c3
	H42	0.140	h1	0.212	h1
	H43	0.140	h1	0.212	h1
	C1	-0.146	c3	-0.404	c3
	H1	0.140	h1	0.212	h1
	H2	0.531	ho	0.417	HW
Water	O	-0.834	OW	-0.834	OW
	H1	0.417	HW	0.417	HW
	H2	0.417	HW	0.292	ha

Calibration			
H_{12}		α	
14.83		-68.02	
Atom Type			
Atom_type	**LJ_Rm**	**LJ_eps**	**SP_Ci**
c1	1.908	0.21	53
ce	1.908	0.086	53
oh	1.72	0.21	53
o	1.66	0.21	50

ho	0.0	0.0	50
HW	0.0	0.0	50
OW	1.768	0.152	90
ha	1.459	0.015	53
Bond Type			
PRM_ID	**D(kcal/mol)**	**alpha**	**r0**
HW-OW	97.2	2.0	0.988
ho-oh	102.0	2.0	0.988
ce-ha	100.0	2.3	1.1

Scheme S10

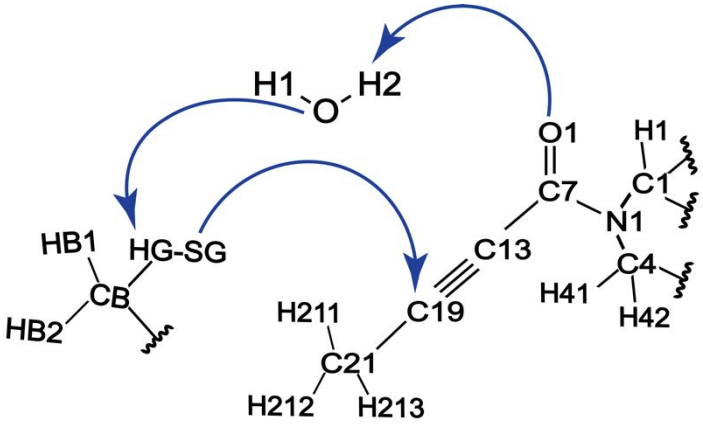

Scheme S10 Figure. The solvent-assisted concerted proton transfers nucleophilic attack step corresponding to scheme S2.

Scheme S10 Table. Atomic charges used for the solvent assisted PT-NA reaction in ITK.

Systems	Atom	RESP charges in RS state	Atom type (RS)	RESP charges in PS state	Atom type (PS)
Cysteine	CB	-0.109	2C	-0.367	c3
	HB1	0.126	H1	0.201	h1
	HB2	0.126	H1	0.201	h1
	SG	-0.414	SH	-0.195	ss
	HG	0.263	HS	0.417	HW
Inhibitor	C21	-0.336	c3	-0.713	c3
	H211	0.189	hc	0.250	hc
	H212	0.189	hc	0.250	hc
	H213	0.189	hc	0.250	hc
	C19	0.316	c1	0.336	c2
	C13	-0.599	cg	-0.351	c1
	C7	0.996	c	0.601	c2
	O1	-0.795	o	-0.717	oh
	N1	-0.057	n	-0.406	nh
	C4	-0.336	c3	-0.146	c3
	H42	0.193	h1	0.140	h1
	H43	0.193	h1	0.140	h1
	C1	-0.336	c3	-0.146	c3
	H1	0.193	h1	0.140	h1
Water	O	-0.834	OW	-0.834	OW
	H1	0.417	HW	0.417	HW
	H2	0.417	HW	0.531	ho

Calibration			
H_{12}		α	
38.98		162.44	
Atom Type			
Atom_type	**LJ_Rm**	**LJ_eps**	**SP_Ci**
SH	2.0	0.25	53
ss	2.0	0.25	91
HS	0.6	0.0157	53

ho	0.0	0.0	53
c1	1.908	0.1	50
c2	1.908	0.086	50
o	1.66	0.21	90
oh	1.72	0.21	50
Bond Type			
PRM_ID	**D(kcal/mol)**	**alpha**	**r0**
HW-OW	97.2	2.0	0.988
HS-SH	94.0	1.4	1.345
ho-oh	102.0	2.0	0.988
c2-ss	90.0	1.2	1.86
Torsion type			
PRM_ID	**FC**	**Mult**	**Psi0**
oh-c2-c1-c2	97.2	2.0	0.988

BTK

Scheme S11

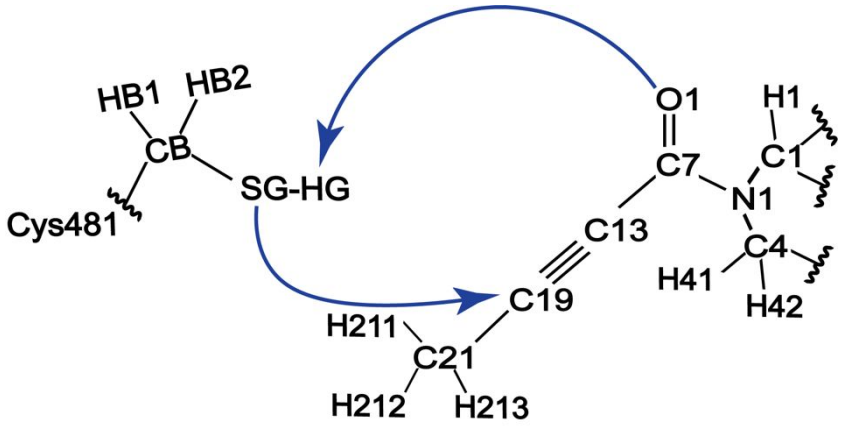

Scheme S11 Figure. The concerted proton transfer-nucleophilic attack (PTNA) step corresponding to scheme S1 (a).

Scheme S11 Table. Atomic charges used for the first proton transfer between cysteine 481to O1 of inhibitor, and the nucleophilic attack between sulfur of cysteine and C19 of inhibitor in BTK.

Systems	Atom	RESP charges in RS state	Atom type (RS)	RESP charges in PS state	Atom type (PS)
Cysteine	CB	-0.116	2C	-0.367	c3
	HB1	0.117	H1	0.201	h1
	HB2	0.117	H1	0.201	h1
	SG	-0.391	SH	-0.195	ss
	HG	0.267	HS	0.531	HO
Inhibitor	C21	-0.336	c3	-0.713	2C
	H211	0.189	hc	0.250	hc
	H212	0.189	hc	0.250	hc
	H213	0.189	hc	0.250	hc
	C19	0.315	c1	0.336	c2
	C13	-0.599	cg	-0.351	c1
	C7	0.996	c	0.601	c2
	O1	-0.795	o	-0.717	oh
	N1	-0.057	n	-0.406	nh
	C4	-0.336	c3	-0.146	c3
	H42	0.193	h1	0.140	h1
	H43	0.193	h1	0.140	h1
	C1	-0.336	c3	-0.146	c3
	H1	0.193	h1	0.140	h1

Calibration			
H_{12}		α	
38.98		162.44	
Atom Type			
Atom_type	**LJ_Rm**	**LJ_eps**	**SP_Ci**
SH	2.0	0.25	30
ss	2.0	0.25	90
HS	0.6	0.0157	50

ho	0.0	0.0	50
c1	1.908	0.1	91
c2	1.908	0.086	91
o	1.66	0.21	90
oh	1.72	0.21	50
Bond Type			
PRM_ID	**D(kcal/mol)**	**alpha**	**r0**
HS-SH	94.0	1.4	1.345
ho-oh	102.0	2.0	0.988
c2-ss	90.0	1.2	1.86

Scheme S12

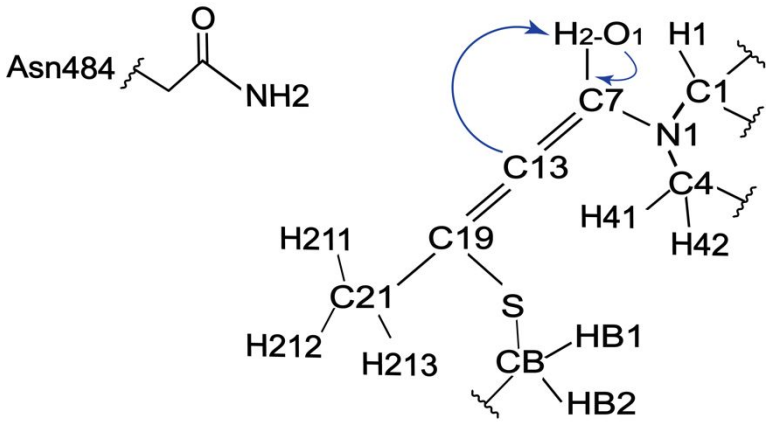

Scheme S12 Figure. The direct tautomerization step corresponding to scheme S1 (a).

Scheme S12 Table. Atomic charges used for tautomerization in BTK.

Systems	Atom	RESP charges in RS state	Atom type (RS)	RESP charges in PS state	Atom type (PS)
CYS	CB	-0.367	c3	-0.278	c3
	HB1	0.201	h1	0.197	h1
	HB2	0.201	h1	0.197	h1
	SG	-0.195	ss	-0.225	ss
inhibitor	C21	-0.713	c3	-0.339	c3
	H211	0.250	hc	0.161	hc
	H212	0.250	hc	0.161	hc
	H213	0.250	hc	0.161	hc
	C19	0.336	c2	0.368	c2
	C13	-0.351	c1	-0.579	ce
	C7	0.601	c2	0.904	c
	O1	-0.717	oh	-0.799	o
	N1	-0.406	nh	-0.051	n
	C4	-0.146	c3	-0.403	c3
	H42	0.140	h1	0.212	h1
	H43	0.140	h1	0.212	h1
	C1	-0.146	c3	-0.406	c3
	H1	0.140	h1	0.212	h1
	H2	0.531	ho	0.292	ha

Calibration			
H_{12}		α	
18.68		-50.95	
Atom Type			
Atom_type	**LJ_Rm**	**LJ_eps**	**SP_Ci**
c1	1.908	0.21	53
ce	1.908	0.086	53
oh	1.72	0.21	53
o	1.66	0.21	50
ho	0.0	0.0	50
ha	1.459	0.015	50
Bond Type			

PRM_ID	D(kcal/mol)	alpha	r0
ho-oh	102.0	2.35	0.960
ce-ha	100.0	2.3	1.1

Scheme S13

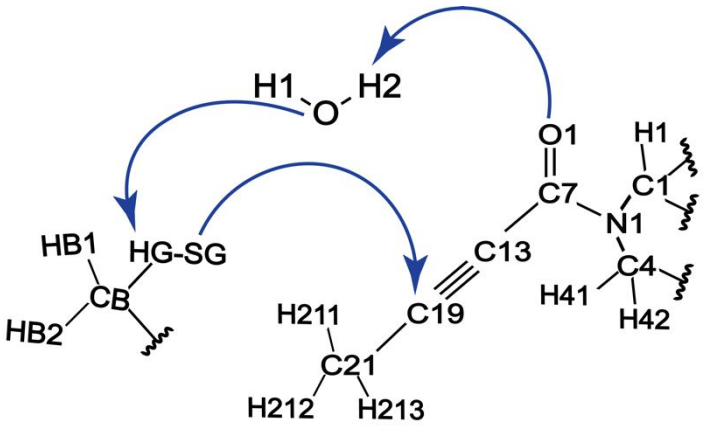

Scheme S13 Figure. The concerted solvent assisted proton transfer-nucleophilic attack (PT-NA) step corresponding to scheme S1 (b).

Scheme S13 Table. Atomic charges used for the first proton transfer between cysteine 481and water, and the nucleophilic attack between sulfur of cysteine and C19 of inhibitor in BTK.

Systems	Atom	RESP charges in RS state	Atom type (RS)	RESP charges in PS state	Atom type (PS)
Cysteine	CB	-0.109	2C	-0.367	c3
	HB1	0.126	H1	0.201	h1
	HB2	0.126	H1	0.201	h1
	SG	-0.414	SH	-0.195	ss
	HG	0.263	HS	0.417	HW
Inhibitor	C21	-0.336	c3	-0.713	c3
	H211	0.189	hc	0.250	hc
	H212	0.189	hc	0.250	hc
	H213	0.189	hc	0.250	hc
	C19	0.316	c1	0.336	c2
	C13	-0.599	cg	-0.351	c1
	C7	0.996	c	0.601	c2
	O1	-0.795	o	-0.717	oh
	N1	-0.057	n	-0.406	nh
	C4	-0.336	c3	-0.146	c3
	H42	0.193	h1	0.140	h1
	H43	0.193	h1	0.140	h1
	C1	-0.336	c3	-0.146	c3
	H1	0.193	h1	0.140	h1
Water	O	-0.834	OW	-0.834	OW
	H1	0.417	HW	0.531	ho
	H2	0.417	HW	0.417	HW

Calibration			
H_{12}		α	
45.41		134.66	
Atom Type			
Atom_type	**LJ_Rm**	**LJ_eps**	**SP_Ci**
SH	2.0	0.25	53
ss	2.0	0.25	91

HS	0.6	0.0157	53
HW	0.0	0.0	53
c1	1.908	0.21	50
c2	1.908	0.086	50
o	1.66	0.21	90
oh	1.721	0.21	50
OW	1.768	0.152	90
ho	0.0	0.0	53
Bond Type			
PRM_ID	**D(kcal/mol)**	**alpha**	**r0**
HW-OW	97.2	2.0	0.988
HS-SH	94.0	1.4	1.345
ho-oh	102.0	2.0	0.988
c2-ss	90.0	1.2	1.86

Scheme S14

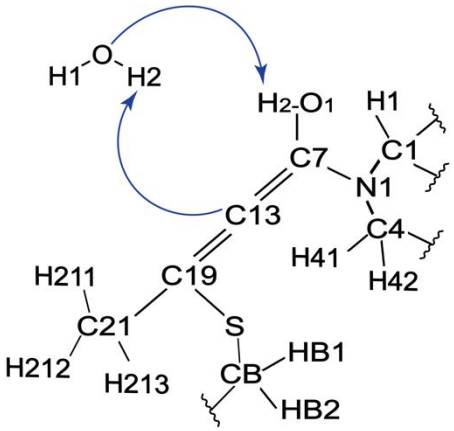

Scheme S14 Figure. The solvent assisted tautomerization step corresponding to scheme S1 (b).

Scheme S14 Table. Atomic charges used for solvent assisted tautomerization in BTK.

Systems	Atom	RESP charges in RS state	Atom type (RS)	RESP charges in PS state	Atom type (PS)
Cysteine	CB	-0.367	c3	-0.278	c3
	HB1	0.201	h1	0.197	h1
	HB2	0.201	h1	0.197	h1
	SG	-0.195	ss	-0.225	ss
Inhibitor	C21	-0.713	c3	-0.339	c3
	H211	0.251	hc	0.162	hc
	H212	0.251	hc	0.162	hc
	H213	0.251	hc	0.162	hc
	C19	0.326	c2	0.367	c2
	C13	-0.351	c1	-0.579	ce
	C7	0.601	c2	0.904	c
	O1	-0.717	oh	-0.799	o
	N1	-0.406	nh	-0.051	n
	C4	-0.146	c3	-0.404	c3
	H42	0.140	h1	0.212	h1
	H43	0.140	h1	0.212	h1
	C1	-0.146	c3	-0.404	c3
	H1	0.140	h1	0.212	h1
	H2	0.531	ho	0.417	HW
Water	O	-0.834	OW	-0.834	OW
	H1	0.417	HW	0.417	HW
	H2	0.417	HW	0.292	ha

Calibration			
H_{12}		α	
47.24		-71.71	
Atom Type			
Atom_type	**LJ_Rm**	**LJ_eps**	**SP_Ci**
c1	1.908	0.086	53
ce	1.908	0.086	53
oh	1.72	0.21	53
o	1.66	0.21	50
ho	0.0	0.0	50

HW	0.0	0.0	50
OW	1.768	0.152	53
ha	1.459	0.015	50
Bond Type			
PRM_ID	**D(kcal/mol)**	**alpha**	**r0**
HW-OW	97.2	2.0	0.988
ho-oh	102.0	2.0	0.988
ce-ha	100.0	2.3	1.1

Reference:

1. Bauer, P. *et al.* Q6: A comprehensive toolkit for empirical valence bond and related free energy calculations. *SoftwareX* **7**, 388–395 (2018).
2. Wang, J., Wolf, R. M., Caldwell, J. W., Kollman, P. A. & Case, D. A. Development and testing of a general amber force field. *Journal of Computational Chemistry* **25**, 1157–1174 (2004).
3. Maier, J. A. *et al.* ff14SB: Improving the Accuracy of Protein Side Chain and Backbone Parameters from ff99SB. *J. Chem. Theory Comput.* **11**, 3696–3713 (2015).
4. Maple, J. R., Dinur, U. & Hagler, A. T. Derivation of force fields for molecular mechanics and dynamics from ab initio energy surfaces. *Proceedings of the National Academy of Sciences* **85**, 5350–5354 (1988).
5. Singh, N. & Warshel, A. Absolute binding free energy calculations: On the accuracy of computational scoring of protein–ligand interactions. *Proteins: Structure, Function, and Bioinformatics* **78**, 1705–1723 (2010).
6. Sham, Y. Y., Chu, Z. T., Tao, H. & Warshel, A. Examining methods for calculations of binding free energies: LRA, LIE, PDLD-LRA, and PDLD/S-LRA calculations of ligands binding to an HIV protease. *Proteins: Structure, Function, and Bioinformatics* **39**, 393–407 (2000).
7. Warshel, A. *et al. Molaris-XG*. (University of Southern California, 2012).
8. Lee, F. S. & Warshel, A. A local reaction field method for fast evaluation of long-range electrostatic interactions in molecular simulations. *J. Chem. Phys.* **97**, 3100–3107 (1992).
9. Wolfram, S. The Mathematica Book (3rd ed.). *Assembly Automation* **19**, 77–77 (1999).

10. Kyte, J. & Doolittle, R. F. A simple method for displaying the hydropathic character of a protein. *J Mol Biol* **157**, 105–132 (1982).

11. Hawkins, J. & Marcy, A. Characterization of Itk Tyrosine Kinase: Contribution of Noncatalytic Domains to Enzymatic Activity. *Protein Expression and Purification* **22**, 211–219 (2001).

12. Dinh, M. *et al.* Activation Mechanism and Steady State Kinetics of Bruton's Tyrosine Kinase *. *Journal of Biological Chemistry* **282**, 8768–8776 (2007).

13. Liclican, A. *et al.* Biochemical characterization of tirabrutinib and other irreversible inhibitors of Bruton's tyrosine kinase reveals differences in on - and off - target inhibition. *Biochimica et Biophysica Acta (BBA) - General Subjects* **1864**, 129531 (2020).